24th COBEM - 2017

24th ABCM International Congress of Mechanical Engineering
December 3-8, 2017, Curitiba, PR, Brazil

COBEM-2017-1008
DYNAMIC ANALYSIS OF A THREE-PHASE REACTOR OF FIXED BED FOR PETROLEUM AND PETROCHEMICAL INDUSTRY

Emerson Barbosa dos Anjos
Jornandes Dias da Silva
Juliana Damasceno da Cruz Gouveia de Carvalho
Polytechnic School – UPE, Environmental and Energetic Technology Laboratory, Recife PE, Brazil
emersonanjos@poli.br ; jornandesdias@poli.br ; juliana.dcgc@hotmail.com

Abstract. *The Fixed-Bed Three-Phase Reactors (FBTRs) are used equipment in the petrochemical and petroleum industries with diverse applications. Effective control of these reactors is critical to secure operations, especially when high performance is desired. In this way, the reactor must be controlled very well and for that, a mathematical model is needed that describe its behavior in the best possible way, being able even to predict its dynamic behavior. In this sense, the present work aims to perform the mathematical modeling of FBTR. To perform the modeling the technique known how coupled integral equation approach was applied to the energy balance equations of the fluid and solid phases, transforming the Partial Differential Equations (PDEs) into Ordinary Differential Equations (ODEs). The results of the work were obtained through the elaboration of software in the language FORTRAN 95, where the Euler method was applied in the ODEs obtaining the graphs for the temperature versus time. In this way, it can be concluded that in this present model the heat transfer coefficient is important for the control of the reactor, being sensitive to changes and that to obtain the time of stabilization of the temperature of the reactor obtaining a control of this reactor and avoiding the formation of hot spots.*

Keywords: *Fixed Bed, Mathematical Model, Heat Transfer, Euler Method.*

1. INTRODUCTION

The Fixed-Bed Three-phase Reactors (FBTRs) are defined by the fluid flow characteristic in the downward concurrent direction across the fixed bed of the particles in the continuous phase. This reactor have been extensively used in hydrotreating, hydrodesulfurization in petroleum refining, petrochemical hydrogenation and oxidation process, and methods of biochemical and detoxification of industrial waster. In this equipment, a liquid film under the surface of the catalyst is formed enabling the gas phase to flow continuously between the catalytic particles. Thus, it is noticeable that the fixed bed hydrodynamics is an important process in the development of mathematical models that describe the interfacial phenomena in the FBTR, such as mass and heat transfer.

Several researchers made great efforts to improve the understanding of the FBTR process of the gaseous and liquid phases. Most of the works are focused on issues such as pressure drop, liquid phase retention, flow distribution, moisture efficiency and fluid phase phenomena. However, few studies are related to the phenomenon of heat transfer in the fluid and solid phases in the fixed bed. In addition, heat transfer in multiphase process for non-isothermal system in TFBR is considered one of the most significant areas of thermal engineering.

The heat transfer in the FBTRs involves the conduction and convection processes. Several researchers in the literature have addressed these themes. Asukuma, *et al, 2017* perfomed a numerical analysis of the effect of thermal conductivity and conduction and thermal radiation on the fixed bed system. They investigated the thermal conductivity to clarify the phenomenon of heat transfer in a fixed bed, defining the number of biot for thermal radiation as a function of temperature, particle size, emissivity and the configuration factor. The authors obtained the results through the homogenization method and showed that the number of Biot and that can simplify the effective thermal conductivity with the thermal radiation even with complexity of the model the thermal behavior in the fixed bed can be expressed as a sigmoidal function with the biot number. Heidari and Hashemabadi (2014) analyzed interfacial heat exchange using a simplified model for a 60 mm internal diameter drip bed reactor with fourteen 40 mm spheres aligned with the spindle axis. In this research, the authors considered the flow of gas flowing concurrently to examine the interfacial Nusselt number as a function of the Reynolds and Prandtl numbers. These authors concluded that there was an increase of the heat transfer with the increase

of Reynolds and Prandtl numbers with respect to the gas phase and the decrease with the numbers of Reynolds, Prandtl and Eötvös with respect to the liquid phase.

Despite having several researches on these reactors, the numerical simulation for the dynamic non-isothermal process is still little studied in the literature based on mathematical models involving the particle equation. As a justification, the complete modeling, combining the intraparticular diffusion effect is quite complex. In this way, in this contribution, the present paper presents a mathematical model formed by coupled equations of the energy balance for the gas-liquid and solid phases in the FBTR.

In this work, a one-dimensional model is presented to mathematically simulate the process of heat transfer in an FBTR. Thus, considering the energy balance equations for the gas-liquid and solid phases in the fixed bed, simulations were performed using the models provided for the heat transfer process by verifying the behavior of the temperatures in the gaseous and solid phases within the FBTR. Finally, the simulations were presented in terms of temperature changes as a function of time by varying the heat transfer coefficient.

2. TEORY OF MATHEMATICAL MODEL

The FBTR are models with concurrent fluid configurations on particles (Fig. 1), they can be considered as an initial value problem (IVP) and in this way, it is possible to estimate their temperature as a function of time. Mathematical models can be used to analyze reactor designs and operating conditions. Thus, the present work presents a one-dimensional model to predict the evolution of temperatures in the gaseous and solid phases

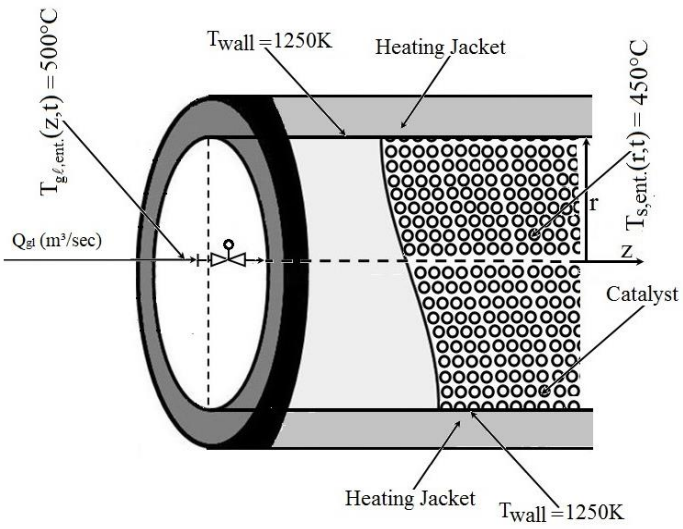

Figure. 1 – Model of a fixed bed three-phase reactor to study the catalytic reform process for fuel production.

Mathematical models are important tools for a science, since they contribute in the identification of the sensitivity of updating a reactor by variations of different operating conditions and the parameters of the project, (Silva, 2012). Due to the geometric complexity of the FBTRs, the transport of fluid in porous media is described by complex mathematical models that must be simplified before their resolution. With the objective of developing a dynamic mathematical model for heat transfer in porous media of the FBTRs proposed in the present article, a temperature of the gaseous and liquid phases was oriented in the axial direction of the reactor and temperature in the continuous phase in the radial direction of the part of the.

The partial differential equations (EDPs) of the developed model are deduced considering an infinitesimal element of the reactor. In order to analyze the thermal variables of the proposed mathematical modeling, the following assumptions were adopted:

i. Temperature gradients in the axial direction of the FBTR were considered.
ii. Temperature gradients in the radial direction of the particles were considered.
iii. The system operates under a dynamic regime.
iv. In the proposed model, only thermal effects were considered in both phases.
v. The wall temperature of the FBTR was considered constant.
vi. Uniform particle size.

Based on the assumptions above, the energy balance equations for the gas phase as well as for the solid phase are given as follows:

- Energy Balance for fluid-phase:

$$\varphi_{gl}\frac{\partial T_{gl}(z,t)}{\partial t}+\vartheta_{gl}\frac{\partial T_{gl}(z,t)}{\partial z}=\mu_{gl}\frac{\partial^2 T_{gl}(z,t)}{\partial z^2}+Q_{gl} \tag{1}$$

Where, $\varphi_{g\ell}$ (Kj/m^{3}K) is the coefficient of the term of thermal accumulation, T_{gl} (K) is the fluid temperature, $\vartheta_{g\ell}$ (kJ/m^{3}K s) is the coefficient of the term of thermal convection , t (s) is the time, z (m) é a coordinate in the axial direction respectively, $\mu_{g\ell}$ (kJ/m^{3}K s) is the coefficient of the term of thermal dispersion , Q_{gl} (m^3/s) is the rate of heat transfer between temperatures, respectively.

- The coefficient of Eq.1, φ_{gl}, ϑ_{gl}, μ_{gl} and Q_{gl} are given by the equations bellow:

$$\varphi_{gl}=h_g\rho_g C_{p,g}+h_l\rho_l C_{p,l}\ ;\ \vartheta_{gl}=\frac{h_g\rho_g C_{p,g}V_{sg}+h_l\rho_l C_{p,l}V_{sl}}{L}\ ;\ \mu_{gl}=\frac{h_g\lambda_g+h_l\lambda_l}{L^2}\ ;\ Q_{gl}=h_{fp}\frac{-3}{r_p}(1-\varepsilon_s)[T_{gl}(z,t)-T_s(r,t)|_{r=R}] \tag{2}$$

Where, h_g (m^3 of gas|m^3 de reactor) is the retention of the gaseous-phase, ρ_g (kg/m^3) is the density of the gaseous-phase, $C_{p,g}$ (kJ/kg K) is heat capacity of the gaseous, h_ℓ (m^3 of liquid/m^3 of reactor) is the retention of liquid-phase, ρ_ℓ (kg/m^3) is the density of liquid phase, $C_{p,\ell}$ (kJ/kg K) is heat capacity of the liquid, respectively; V_{sg} (m/s) is the surface speed of the gaseous phase, $V_{s\ell}$ (m/s) is the surface speed of the liquid phase, L (m) is the bed length, λ_g (kJ/m K s) is the thermal conductivity for the gaseous phase, λ_ℓ (kJ/m K s) is the thermal conductivity for the liquid phase, , h_{fp} (kJ/m^{2}K s) is the coefficient of heat transfer in fluid-particle, r_p (m) radius of particle, ε_b (m^3 of fluid/m^3 of reactor) is the bed porosity, T_s (K) is the temperature of solid phase, respectively.

- Initial and boundary conditions for the Eq (1)

$$T_{gl}(z,0)=T_{gl},0\ ;\ T_{gl}(z,0)\in(0,L)\ e\ T_{gl}(z,0)\in(t_0,t_{final}) \tag{3}$$

$$\left.\frac{\partial T_{gl}(z,t)}{\partial z}\right|_{z=0^+}=\frac{\vartheta_{gl}}{\mu_{gl}}T_{gl}(0,t)-\frac{\vartheta_{gl}}{\mu_{gl}}T_{gl},0 \tag{4}$$

$$\left.\frac{\partial T_{gl}(z,t)}{\partial z}\right|_{z=L}=0\quad ;\quad para\ t\geq 0 \tag{5}$$

- Energy Balance for solid-phase:

$$\rho_s C_{p,s}\frac{\partial T_s(r,t)}{\partial t}=\frac{\lambda_s}{R^2}\frac{1}{r^2}\frac{\partial}{\partial r}\left[\frac{r^2\partial T_s(r,t)}{\partial r}\right] \tag{6}$$

Where, ρ_s(kg/m^3) is the density of the solid phase, $C_{p,s}$(kJ/kg·K) is the heat capacity of the solid phase, respectively; λ_s (kJ/m K s) is the termal conductivity for the solid phase, R (m) is the superficial radius of the solid phase, r (m) is the particle radius,, respectively.

- Initial and boundary conditions for the Eq (6)

$$T_s(z,0)=T_{s,0};T_s(z,0)\in(0,L)\ e\ T_s(z,0)\in(t_0,t_{final}) \tag{7}$$

$$\lambda_s\left.\frac{\partial T_s(z,t)}{\partial r}\right|_{r=R}=h_{fp}\left[T_{g\ell}-T_s|_{r=R}\right] \tag{8}$$

$$\left.\frac{\partial T_s(z,t)}{\partial r}\right|_{r=0^+} = 0 \tag{9}$$

3. SOLUTION STRATEGY

Before the creation of the computer, solutions to physical problems, such as heat transfer or drainage, were performed exclusively by analytical methods. However, from the advance of computer science, the use of numerical methods became widespread and it became possible to obtain better solutions to the problems of engineering. But, analytical solutions are still essential in the development of science and engineering, and their relevance should not be ignored. (Reis and Chaves, 2010).

The Hermite approximation is to approximate an integral through a linear combination of integrand values and derivatives thereof. It was originally developed by Hermite (1878) and first presented by Menning, *et al*, 1983. These approximations allow a complex problem to be simplified, so that it can be solved with much less effort, and in many cases using analytical methods. The advantage of this technique, when compared to the traditional method of approximations, is that a smaller error is found, making it possible to obtain a good precision of the results. In addition, several researchers have already studied this technique: Cardoso, *et al*, 2014, Knupp, *et al*, 2012, An and Su (2011), Corrêa and Cotta (1998) and among others.

This technique, based on Hermite approximation, was called Coupled Equation Integral Approach (CEIA). In this paper, to transform the equations differential partial (EDPs) of the energy balance (Eqs 1a and 1b) in equations differential ordinary (EDOs) the CEIA was used. In addition, to solve this EDOs the Euler method was applied with one software in language FORTRAN 95. In this way, a study of fluid and solid phase temperature of RFLT over time was obtained.

3.1 Hermite approximation

The basis of the approximation by coupled integrals is the Hermite approximation for integrals, originally developed by Hermite (1878). Under the following form:

$$\int_{x_{i-1}}^{x_i} y(x)dx = \sum_{v=0}^{\alpha} C_v y_{i-1}^{(v)} + \sum_{v=0}^{\beta} D_v y_i^{(v)} \tag{10}$$

Where y(x) and its derivatives $y^{(v)}(x)$ are defined for all $x \in (x_{i-1},x_1)$.Furthermore it is assumed that the numerical values of $y^{(v)}(x_{i1}) \equiv y_{i-1}^{(v)}$ for v = 0,1,2,3...,α and $y^{(v)}(x_i) \equiv y_i^{(v)}$ para v = 0,1,2,3,..., β are available at the end points of the interval.

In such a manner the integral of y(x) is expressed as a linear combination of (x_{i-1}), $y(x_i) \equiv y_{i-1}^{(v)}$ and their derivatives, $y^{(v)}(x_{i-1})$ up to order v = α e $y^{(v)}(x_i)$ up to order de v = β. Therefore, this is called the $H_{\alpha,\beta}$ approximation. The resulting expression for this approximation is given by:

$$\int_{x_{i-1}}^{x_i} y(x)dx \cong \sum_{v=0}^{\alpha} C_v(\alpha,\beta) h_i^{v+1} y_{i-1}^{(v)} + \sum_{v=0}^{\beta} C_v(\alpha,\beta)(-1)^v h_i^{v+1} y_i^{(v)} + O(h_i^{\alpha+\beta+3}) \tag{11}$$

Where,

$$h_i = x_i - x_{i-1};\ C_v(\alpha,\beta) = \frac{(\alpha+1)!(\alpha+b+1-v)!}{(v+1)!(\alpha-v)!(\alpha+\beta+2)!} \tag{12}$$

3.2 $H_{1,1}|H_{0,0}$ solution

To solve the equations of the proposed energy balances through the CIEA, the following equations are used:

$$\bar{T}_n(t) \cong \frac{L}{2}[T_n(0,t) + T_n(L,t) + \frac{L}{12}\left[\left.\frac{\partial T_n}{\partial s}\right|_{s=0} - \left.\frac{\partial T_n}{\partial s}\right|_{s=L|R}\right] \tag{13}$$

$$T_n(L,t) - T_n(0,t) \cong \frac{L}{2}\left[\left.\frac{\partial T_n}{\partial s}\right|_{s=0} + \left.\frac{\partial T_n}{\partial s}\right|_{s=L|R}\right] \tag{14}$$

Based on the above equations, the initial and boundary conditions are applied and obtain the expresssions $T_{gl}(0,t)$, $T_{gl}(1,t)$ e $T_s(0,t)$, $T_s(1,t)$.Then, apply the operator $\int dx$ with limites 0 and 1 and thought the following definition,

$$\int_0^1 T_{gl}(z,t)dz = T_{gl}(t) \tag{15}$$

$$\int_0^1 \frac{\partial T_{gl}(z,t)}{\partial z} dz = T_{gl}(1,t) - T_{gl}(0,t) \tag{16}$$

$$\int_0^1 T_s(r,t)dr = T_s(t) \tag{17}$$

$$\int_0^1 \frac{\partial T_s(r,t)}{\partial r} dr = T_s(1,t) - T_s(0,t) \tag{18}$$

And the expressions mentioned above it is possible to obtain the following ODE's

$$\frac{d\overline{T}_{g\ell}(t)}{dt} = \alpha_{5,g\ell}(T_{g\ell},0) - \alpha_{7,g\ell}\overline{T}_{g\ell}(t) + \alpha_{6,g\ell}\overline{T}_s(t) \tag{19}$$

$$\frac{d\overline{T}_s(t)}{dt} = \beta_{6,s}\,\alpha_{4,gl}(T_{gl},0) + \beta_{6,s}\alpha_{3,gl}\overline{T}_{g\ell}(t) - \beta_{7,s}\,\overline{T}_s(t) \tag{20}$$

The parameter $\alpha_{3,g\ell}$, $\alpha_{4,g\ell}$, $\alpha_{5,g\ell}$, $\alpha_{6,g\ell}$, $\alpha_{7,g\ell}$, $\beta_{6,s}$, $\beta_{7,s}$ e $\beta_{8,s}$ are obtain through the mathematical deduction (Tab.1).

Table 1 - Parameters of mathematical deduction of Eqs. 19 and 20.

$\alpha_{1,g\ell} = \left(\frac{3\mu_{g\ell} + \vartheta_{g\ell}}{3\mu_{g\ell}}\right)$	$\alpha_{43,g\ell} = \left[-\frac{1}{2}\frac{\vartheta_{g\ell}}{\mu_{g\ell}}\right]$	$\beta_{2,s} = \left(\frac{1}{3}\frac{h_{fp}}{\lambda_s}\right)$
$\alpha_{2,g\ell} = \frac{1}{3}\frac{\vartheta_{g\ell}}{\mu_{g\ell}}$	$\alpha_{5,g\ell} = \frac{(\vartheta_{g\ell} - \vartheta_{g\ell}\,\alpha_{4,g\ell})}{\varphi_{g\ell}}$	$\beta_{3,s} = \left[-\frac{h_{fp}}{2\lambda_s} + \left(\frac{h_{fp}}{2\lambda_s} + 1\right)\frac{\beta_{2,s}}{\beta_{1,s}}\right]$
$\alpha_{3,g\ell} = \left(\frac{1}{2}\frac{\vartheta_{g\ell}}{\mu_{g\ell}} + 1\right)\frac{1}{\alpha_{1,g\ell}}$	$\alpha_{6,g\ell} = \frac{h_{fp}}{\varphi_{g\ell}}\frac{3}{r_p}(1-\varepsilon_s)$	$\beta_{4,s} = \left[\left(\frac{h_{fp}}{2\lambda_s} + 1\right)\frac{1}{\beta_{1,s}}\right]$
$\alpha_{4,g\ell} = \lfloor \alpha_{42,g\ell} + \alpha_{43,g\ell} \rfloor$	$\alpha_{7,g\ell} = \frac{\vartheta_{g\ell}\,\alpha_{3,g\ell}}{\varphi_{g\ell}} + \alpha_{6,g\ell}$	$\beta_{5,s} = \left(\frac{3}{\rho_s C_{p,s}}\frac{\lambda_s}{R^2}\frac{h_{fp}}{k_s}\right)$
$\alpha_{42,g\ell} = \left(\frac{1}{2}\frac{\vartheta_{g\ell}}{\mu_{g\ell}} + 1\right) \times \left(\frac{\alpha_{2,g\ell}}{\alpha_{1,g\ell}}\right)$	$\beta_{1,s} = \left(\frac{3\lambda_s + h_{fp}}{3\lambda_s}\right)$	$\beta_{6,s} = \left(\beta_{5,s} - \beta_{5,s}\frac{\beta_{2,s}}{\beta_{1,s}}\right)$
		$\beta_{6,s} = \left(\beta_{5,s} - \beta_{5,s}\frac{\beta_{2,s}}{\beta_{1,s}}\right)$

4. RESULTS AND DISCUSSION

A dynamic mathematical model was developed to analyze the temperature variations (T_{gl}) in the gas-liquid phases, as well as the temperature (T_s) in the solid phase in an FBTR. The values of the parameters used in the simulation to obtain temperature evolutions (T_{gl}, T_s, respectively) are given in Tab. 2. In addition, the authors to solve the set of equations mentioned in this work elaborated a computational code (in the FORTRAN 95 language). As results, this table presents in detail all the conditions to simulate the proposed model.

Table 2 - Entry data for the simulation

Categories	Symbol	Number value	Categories	Symbol	Number value
Condition of Operations	$T_{g\ell,0}$	550	Properties of Liquid phase	$C_{p,\,l}$	2,001
	$T_{s,0}$	450		h_ℓ	0,791
	L	1,0		$V_{s,\ell}$	2,01
	ε_s	0,59		λ_l	$1{,}80\text{x}10^{-2}$
	r_p	$3{,}2\text{x}10^{-4}$		ρ_L	$1{,}01\text{x}10^{-2}$
	R	1,0			
Properties of Gaseous phase	$C_{p,\,g}$	$2{,}101\text{x}10^{-1}$	Properties of Solid phase	$C_{p,\,s}$	$2{,}00\text{x}10^{3}$
	h_g	0,80		h_{fp}	$2{,}635\text{x}10^{-2}$
	$V_{s,\,g}$	$29{,}46\text{x}10^{-1}$		λ_s	$1{,}559\text{x}10^{+2}$
	λ_g	0,0547		ρ_s	$1{,}08\text{x}10^{-1}$
	ρ_G	$0{,}933\text{x}10^{-2}$			

Figure 2 shows the evolutions of T_{gl} (K) using the formulation $H_{1,1}|H_{0,0}$. As can be seen in the graph, a dashed region was enlarged according to Fig. 2b within Fig. 2a. Figure 2a shows an energy transfer from the gas-liquid phases to the solid phase in a time interval of $1 \leq t \leq 2.5$s according to Fig. 2b. This phenomenon, happens in the reform processes, with endothermic chemical reaction, for fuel gas production and can be found in Cruz and Silva (2017).

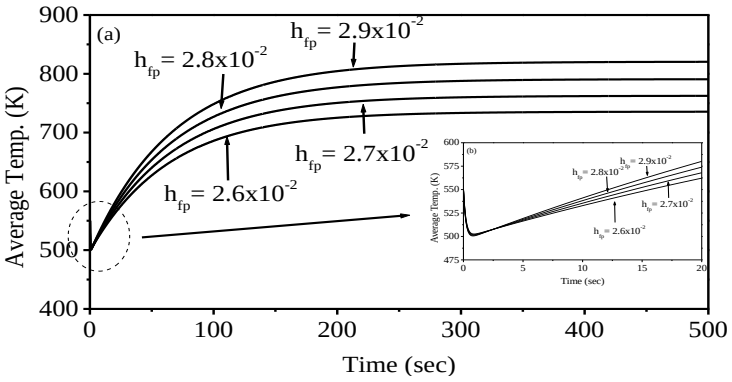

Figure 2 - Evolution of average fluid phase temperature versus time, with analyzes of sensitivity of the parameter, h_{fp}.

In addition, Fig. 2 reports the effect of h_{fp} on the evolutions of T_{gl}(K). For comparison purposes, four different values of h_{fp} on T_{gl}(K) were shown. Fig. 2a presents the approximation of $H_{1,1}|H_{0,0}$ with the hatched region of magnification (Fig. 2b). It was observed that the variation of the h_{fp} between $0 \leq t \leq 3$s on the evolutions of T_{gl}(K) is practically null. The effect of h_{fp} becomes clear, on T_{gl} (K), as time increases. In addition, T_{gl}(K) increases as we increase h_{fp} according to the graph of Fig. 2b. On the other hand, the stable levels of the curves are reached around 350s starting from the initial state.

Starting from the same idea of the previous figure as fig. 3c reports the effect of h_{fp} on the evolutions of T_s(K) to the approximation $H_{1,1}|H_{0,0}$. For comparison purposes, four different values of h_{fp} over T_s(K) were reported. Based on the results of this figure, the effect of h_{fp}, in the first seconds, can be considered null. The effect of h_{fp} on T_s(K) becomes clear as time increases. As seen in Fig. 3d, as the h_{fp} grows, so does the temperature. The evolutions of T_s(K) reach the stable levels around 400s starting from the initial state.

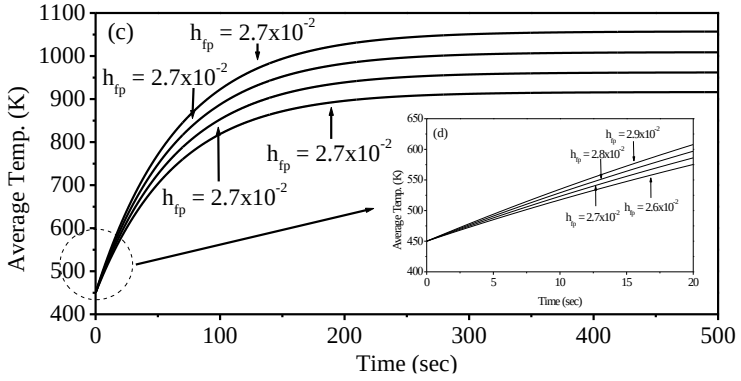

Figure 3 - Evolution of average solid phase temperature versus time with analyzes of sensitivity of the parameter, h_{fp}.

To be clear the variation (Fig. 2 and 3) of the temperature throughout the process with different values of h_{fp} the Tab. 3 below shows all these variations:

Table 3 - Temperature evolution (at 500s) in different h_{sc}.

h_{sc}	T_0 (K) solid	T_0 (K) fluid	$T_{gl\text{-}final}$	$T_{s\text{-}final}$
$2.9x10^{-2}$	450	550	735,47	916,17
$2.8x10^{-2}$	450	550	762,45	961,85
$2.7x10^{-2}$	450	550	790,75	1008,74
$2.6x10^{-2}$	450	550	820,38	1056,86

Figure 4 shows the temperature variation of the solid and gaseous-liquid (fluid) phases over time in the reactor process. It is noticed that in the first seconds the temperature of the fluid is bigger, but near the 20sec the temperature of the solid phase increases and becomes bigger, also a greater heating with respect to the fluid phase is perceived, because while the T_{gl} stabilizes around of the 300sec to T_s stabilizes around the 400sec. In addition, it is noted that the solid phase is important in controlling the reactor.

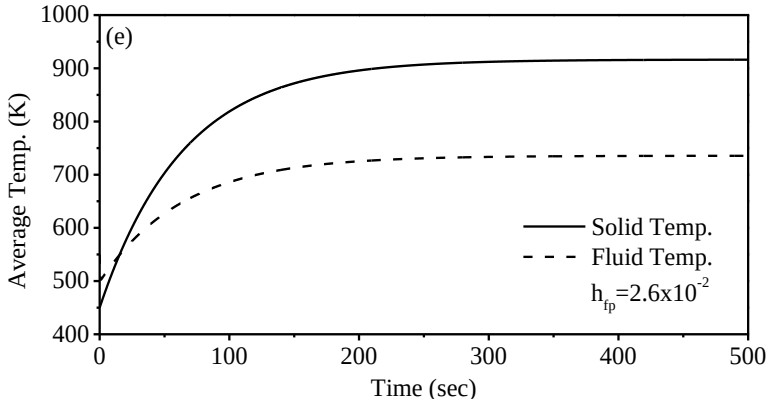

Figure.4 - Variation of solid and fluid temperature over time for $h_{fp} = 2.6x10^{-2}$.

Figure 5f shows the rate of heat transfer between temperatures (Q_{gl}) versus time in the reactor. In the first few seconds a Q_{gl} presents a decreasing behavior because of the energy transfer that is mentioned in fig 2. But throughout the process it is possible to notice a stabilization around the 400sec, near the stabilization of the temperature of the solid phase, realizing, plus one time, that the temperature of this phase is predominant in the control of the reactor. In addition, four h_{fp} values were chosen to show the influence of this parameter throughout the process. In the first 10sec the temperature variation with different h_{fp} was practically nil (Fig. 5g), being remarkable only from the 20seconds. It can also be concluded that as the h_{fp} increases the Q_{gl} increases.

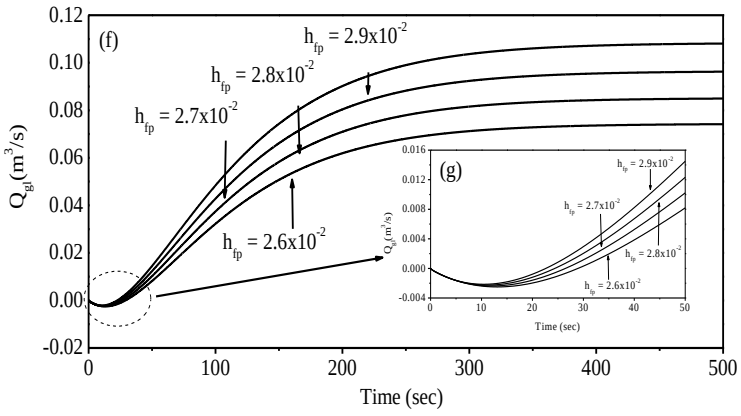

Figure 5 - Evolution of Q_{gl} over the time with analyzes of sensitivity of the parameter, h_{fp}.

5. CONCLUSIONS

The processes of heat transfer in RLFTs are of great importance due to the disadvantage of these equipment in controlling the heat of the exothermic reactions. For, the uncontrolled release of heat from these reactions may generate hot-spots in the reactor bed. The operation of this equipment follows the behavior of the gas-liquid and solid phase temperatures is shown in Figs. 2-4, respectively. In these figures, temperatures versus time were shown to reach their stability levels, especially for the definition of control strategies and / or optimized reactor operations. Thus, it can be concluded that the behavior is defined as the evolution of these temperatures from the input value until reaching the stability conditions of these temperatures.

The development of computer code for analyze the behavior of the variables in this research allowed the lead the following conclusions:

- In the model for the FBR the temperature of the solid phase reaches higher values in relation to the fluid phase (Fig.4) ;
- The developed model allowed the analysis of the temperatures with the variation of parameter h_{sc} (Figs. 2 to 5);
- The studied parameter, h_{sc}, presented huge influence on the variables of the case the higher the coefficient value the higher the temperature (Fig. 2 and 3), also influencing the behavior of the study of the flow (Fig. 5)
- For small intervals, the change in the value of the h_{sc} does not influence in the behavior of the studied variables (T_s, T_{gl}, Q_{gl}).

6. ACKNOWLEDGEMENTS

The authors of this paper would like to thank the CNPQ (National Council for Scientific and Technological Development) for their financial support.

7. REFERENCES

Asakuma, Y. and Honda, I. 2017 “Numerical analysis of effective thermal conductivity with thermal conduction and radiation in packed bed”. *Int. J. of Heat and Mass Transfer*, Vol. 114, p. 402-406.

An, C. and Su, J. 2011 “Improved lumped models for transient combined convective and radiative colling of multi-layer composite”. *Applied Thermal Engineering*, Vol. 31, p.2508-2517.

Cardoso, S.A., Macêdo, E.N. and Quaresma, J.N.N., 2014. “Improved lumped solutions for mass transfer analysis in membrane separation process of metals”. *Int. J. of Heat and Mass Transfer*, Vol. 68, p. 599-611.

Corrêa, E.J. and Cotta R.M. 1998. “Enhanced lumped differential formulations of diffusion problems”. *Applied Mathematical Modelling*, Vol. 22, p. 137-152.

Cruz, B.M. and Silva, J.D. 2017. “A two-dimensional mathematical model for the catalytic steam reforming of methane in both conventional fixed-bed and fixed-bed membrane reactors for the production of hydrogen”. *Int. J. of Hydrogen Energy*, Vol. 42, p. 23670-23690.

Heidari, A. and Hashemabadi, S.H. 2013. “Numerical evaluation of the gas-liquid interfacial heat transfer in the trickle flow regime of packed beds at the micro and meso-scale”. *Chemical Engineering Science*, Vol.104, p.674-689.

Knupp, D.C., Naveira-Cotta, C.P., Ayres, J.V.C, Cotta R.M. and Orlande, H.R.B. 2012. “Theoretical experimental analysis of heat transfer in nonhomogeneous solids via improved lumped formulation, integral transforms and infrared thermography”. *Int. J. of Thermal Sciences*, Vol. 46, p. 878-889.

Reis, M.C., Chaves, M.S. and Sphaier, L.A. 2010. “Technique of coupled integral equations for the calculation of coefficients of friction in laminar flow in ducts and in boundary layer”. In *VI national congress of mechanical engineering - CONEM2010.* Paraiba, Brazil.

Silva, J.D. 2012. 2012. “Dynamic modelling for a trickle-bed reactor using the numerical inverse laplace transform technique. *Procedia Engineering*, Vol.42, p.454-470.

8. RESPONSIBILITY NOTICE

The authors (E.B. Anjos, J.D. Silva and J.D.C.G. Carvalho) are the only responsible for the printed material included in this paper.